Simulations Comparing the Sensitivity of the nlCWFS with the SHWFS

Mala Mateen
Air Force Research Laboratory, Kirtland AFB, NM, 87117
Olivier Guyon
Subaru Telescope, Hilo, HI, 96720
John Codona,
Steward Observatory, Tucson, AZ, 85721

Abstract: We are developing a highly sensitive non-linear Curvature Wavefront Sensor (nlCWFS) which will make it possible to detect objects as dim as m_v 14. In this paper we present a WFS sensitivity comparison between the nlCWFS and the SHWFS based on the ability of each WFS to reconstruct a Fourier mode, given a set signal to noise ratio. Theoretical calculations [1] [2] show that the nlCWFS increases the contrast between a host star and an orbiting planet by two orders of magnitudes. We present simulations that substantiate the theory and show that the nlCWFS can detect an object that is at least two visible magnitudes dimmer than is currently possible with the SHWFS. Since the nlCWFS operates in the photon noise limit it does not require the use of a laser guide star (LGS). We have identified two potential optical designs for the nlCWFS. Over the next year a single design will be selected to integrate the nlCWFS with the AFRL/RDS Optics Division 1.5 m telescope.

1. INTRODUCTION

The non-linear Curvature Wavefront Sensor (nlCWFS) measures intensity in four Fresnel planes on either side of the pupil plane in order to reconstruct the wavefront in the pupil plane [3] [4]. Every spatial frequency present in the wavefront is converted to intensity at a corresponding distance [2]. By effectively samples the distance between the pupil plane and the focal plane the nlCWFS is able to reconstruct both low and high spatial frequencies. The planes closest to the pupil represent high spatial frequencies and the planes further away from the pupil represent low spatial frequencies.

The nlCWFS is sensitive to both low and high spatial frequencies as it is able to interfere all points in its aperture, closely spaced points as well as points separated by the diameter of the aperture. The Shack Hartmann Wavefront Sensor (SHWFS) is limited to interfering points that fall with in a subaperture, making it less sensitive to low spatial frequencies. This can be understood by considering a low spatial frequency like tip-tilt. The SHWFS averages the lateral displacement of the PSF spots across all the subapertures to obtain a global tilt measurement across the aperture. The SH subapertures are typically the size of an r_0 which results in $\frac{\lambda}{r_0}$ PSF spots, across the subaperture. Here r_0 is Fried's parameter which gives the atmospheric coherence length and λ is the sensing wavelength. It is much less sensitive to record the central displacement of a $\frac{\lambda}{r_0}$ spot across an r_0 sized subaperture than it is to record the central displacement of a $\frac{\lambda}{D}$ spot across the aperture, D. The nlCWFS does precisely this, it measures tip-tilt as a displacement of a cloud of $\frac{\lambda}{D}$ speckles across the telescope aperture, D. This results in the nlCWFS having a resolution which is $\frac{D}{r_0}$ times, and a gain that is $(\frac{D}{r_0})^2$ times, higher than the SHWFS.

A large number of actuators are needed to correct a large number of modes and a corresponding number of SH subapertures are need to sense the modes, at least 4 subapertures across a wave are required to accurately sense it and tell its shape and sign . This results in SH subapertures that are smaller than r_0 which further exacerbates the photon noise problem as the size of the PSF spot per subaperture increases yet the number of available photons across each subaperture remains the same. A trade-off has to be made when sensing with the SHWFS, between either obtaining high resolution, or going dim. Once this trade-off is made the SHWFS still suffers from doing a poor job of sensing low order modes due to its lack of spatial coherence. The nlCWFS on the other hand does not split the incident photons in to subapertures and therefore does not suffer from the photon noise problem. The nlCWFS uses the full spatial

Report Documentation Page			*Form Approved* *OMB No. 0704-0188*

1. REPORT DATE	2. REPORT TYPE	3. DATES COVERED
SEP 2014		**00-00-2014 to 00-00-2014**

4. TITLE AND SUBTITLE	
Simulations Comparing the Sensitivity of the nlCWFS with the SHWFS	5a. CONTRACT NUMBER
	5b. GRANT NUMBER
	5c. PROGRAM ELEMENT NUMBER
6. AUTHOR(S)	5d. PROJECT NUMBER
	5e. TASK NUMBER
	5f. WORK UNIT NUMBER
7. PERFORMING ORGANIZATION NAME(S) AND ADDRESS(ES) **Air Force Research Laboratory,Kirtland AFB,NM,87117**	8. PERFORMING ORGANIZATION REPORT NUMBER
9. SPONSORING/MONITORING AGENCY NAME(S) AND ADDRESS(ES)	10. SPONSOR/MONITOR'S ACRONYM(S)
	11. SPONSOR/MONITOR'S REPORT NUMBER(S)

12. DISTRIBUTION/AVAILABILITY STATEMENT

Approved for public release; distribution unlimited

13. SUPPLEMENTARY NOTES

In the Advanced Maui Optical and Space Surveillance Technologies (AMOS) Conference, 9-12 Sep 2014, Maui, HI.

14. ABSTRACT

We are developing a highly sensitive non-linear Curvature Wavefront Sensor (nlCWFS) which will make it possible to detect objects as dim as mv 14. In this paper we present a WFS sensitivity comparison between the nlCWFS and the SHWFS based on the ability of each WFS to reconstruct a Fourier mode, given a set signal to noise ratio. Theoretical calculations [1] [2] show that the nlCWFS increases the contrast between a host star and an orbiting planet by two orders of magnitudes. We present simulations that substantiate the theory and show that the nlCWFS can detect an object that is at least two visible magnitudes dimmer than is currently possible with the SHWFS. Since the nlCWFS operates in the photon noise limit it does not require the use of a laser guide star (LGS). We have identified two potential optical designs for the nlCWFS. Over the next year a single design will be selected to integrate the nlCWFS with the AFRL/RDS Optics Division 1.5m telescope.

15. SUBJECT TERMS

16. SECURITY CLASSIFICATION OF:			17. LIMITATION OF ABSTRACT	18. NUMBER OF PAGES	19a. NAME OF RESPONSIBLE PERSON
a. REPORT **unclassified**	b. ABSTRACT **unclassified**	c. THIS PAGE **unclassified**	**Same as Report (SAR)**	**7**	

coherence of the pupil making it sensitive to both low and high spatial frequencies.

The atmosphere is dominated by low spatial frequencies that scatter light at small angular separations obscuring planets around bright stars. High contrasts between the host star and orbiting planet need to be obtained in order to detect the planet. This requires the ability to resolve and sense low spatial frequencies and obtain a high contrast ratio within a small angular resolution of the central PSF core. We propose the highly sensitive nlCWFS to detect dim object in close proximity to bright targets. In this paper we present simulations carried out for a 1.5 telescope. We compare the sensitivity of the nlCWFS with a SHWFS comprising of 16 and 24 subapertures.

2. Reconstruction and Fourier Decomposition

A Gerchberg-Saxton [5] iterative loop is used to reconstruct the phase sensed with the nlCWFS. The nlCWFS records intensity in four Fresnel planes on either side of the pupil plane. Since we can not measure phase with a sensor the Gerchberg-Saxton loop has no phase information at Fresnel plane (FP) 1, it assumes zero phase. Complex field 1 is constructed using the square root of the recorded intensity in FP 1 and zero phase. Complex field 1 is then propagated to FP 2 and acquires some phase, PH 1 as a result of the propagation. Phase PH 1 is saved. Complex field 1 also has a new amplitude after the propagation, this amplitude is thrown away. Complex field 2 is constructed by using the square root of the intensity recorded at FP 2 and PH 1. Complex field 2 is propagated to FP 3, again the propagation acquired amplitude is thrown away and the phase PH 3 is stored. Complex field 3 is created from the square root of the intensity recorded in FP 3 and PH 3. The process is repeated at FP 4 and Complex filed 4 is created which is then propagated back to the pupil plane. At the pupil plane a flat amplitude constraint is applied and a complex field is created from this flat amplitude plus the propagated phase. The loop repeats as the complex field is propagated to FP 1. The loop repeats till the solution converges and we have reconstructed the pupil plane wavefront. An illustration of the Gerchberg-Saxton loop is shown in Figure 1. The amplitude and the phase are shown at the four Fresnel planes for the twentieth iteration of the Gerchberg-Saxton loop. The pupil plane phase, the reconstructed phase, and their residual is also shown. The flat residual indicates how good the reconstruction is. The SHWFS reconstruction is performed by determining gradients based on the central PSF spot displacement within a subaperture; a reconstruction matrix is computed based on the gradients. Phase reconstruction with the 16 subaperture SHWFS is shown in Figure 2 and with the 24 subaperture SHWFS is shown in Figure 3.

The performance of a wavefront sensor depends on how well it can sense a wavefront. Two criteria define sensor sensitivity, one resolution and, two performance in photon starved conditions. A high resolution sensor should be able to sense a range of spatial frequencies, sampling four pixels per wave or better. A highly sensitive sensor should be able to reconstruct a spatial frequency in a photon noise limited regime. In this paper we compare the sensitivity of the nlCWFS with the SHWFS by determining how well each WFS can reconstruct a Fourier mode. We choose Fourier modes over Zernike modes as the former provides a more fundamental representation of the atmospheric turbulence. This can be understood by considering the relationship between the pupil plane and the focal plane. Each spatial frequency present in the pupil plane has a corresponding intensity representation in the focal plane. Fourier modes, or sine and cosine waves in the pupil plane have a direct relationship to the intensity measured in the focal plane. No such correlation exists for Zernike modes. One draw back, however of using Fourier modes is that they are not orthogonal on a circular aperture, like Zernike modes are. Since Fourier modes do not form an orthogonal basis set on a circular aperture, the basis cannot be inverted by straightforward matrix inversion methods. Singular Value Decomposition (SVD) has to be performed to compute a pseudo-inverse of the Fourier basis set. SVD does a pretty good job of generating an alternate basis set that has orthogonal columns but it does not completely eliminate mode coupling as is shown in section 3. Mode coupling is particularly complex in the case of the nlCWFS due to the non-linear interaction of the modes.

The number of Fourier modes used to reconstruct the wavefront depends on the number of pixels across the WFS. According to Nyquist sampling we want a minimum of two pixels per r_0 which means the number of pixels across the WFS should be at least twice the number of r_0s across your pupil. For the nlCWFS any pixel size can be chosen depending on the size of the r_0s that need to be corrected. This allows the nlCWFS to sense the full range of spatial frequencies required to reconstruct the wavefront. For the AFRL/RDS Optics Division 1.5 m telescope two options are available for the SHWFS, a 16 subaperture and 24 subaperture sensor. The 16 subaperture SHWFS can sense 4 cycles per aperture (cpa) with high resolution and the 24 subaperture SHWFS can sense 6 cpa with high resolution.

The Fourier basis set is generated considering all orientations of the sine and cosine waves that form a cycle per

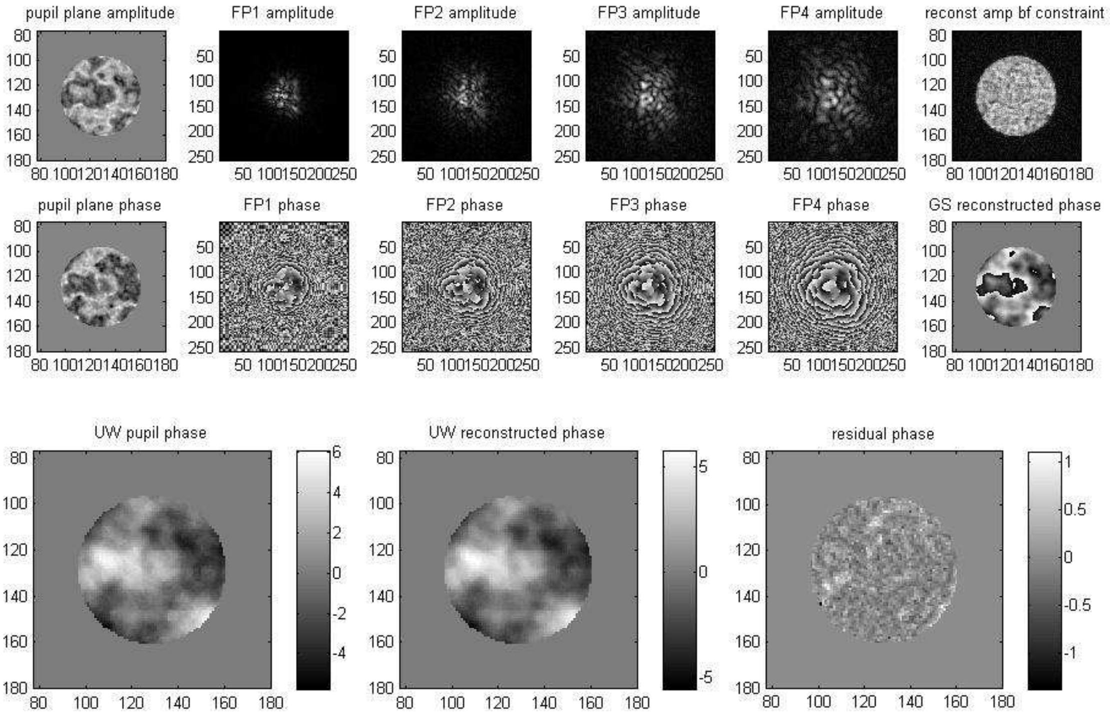

Fig. 1. nlCWFS Gerchberg-Saxton reconstruction. The top row shows the amplitude in the pupil and at each of the Fresnel planes. The middle row shows the phase in the pupil and in each of the Fresnel planes. The third row shows the input phase, the reconstructed phase and the residual between the two. Reconstruction after 20 iterations of the Gerchberg-Saxton loop is shown.

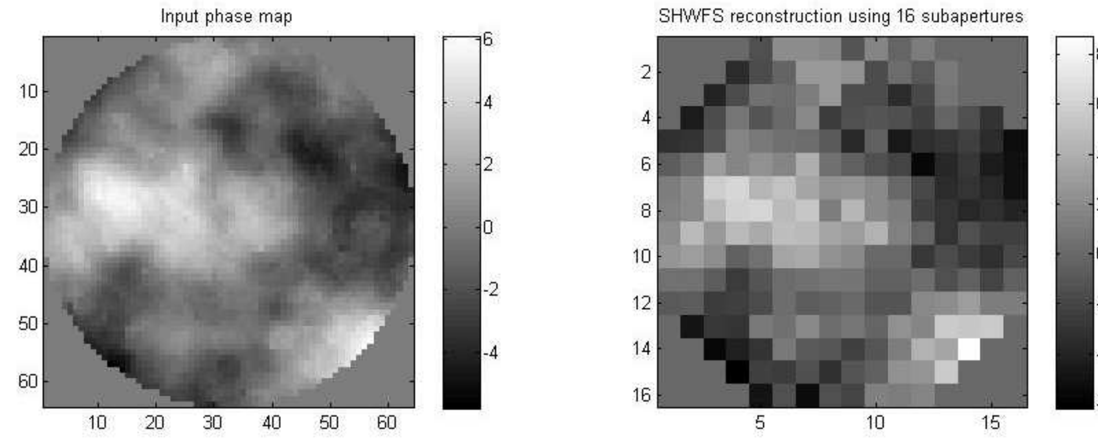

Fig. 2. Wavefront reconstruction using a 16 subaperture SHWFS.

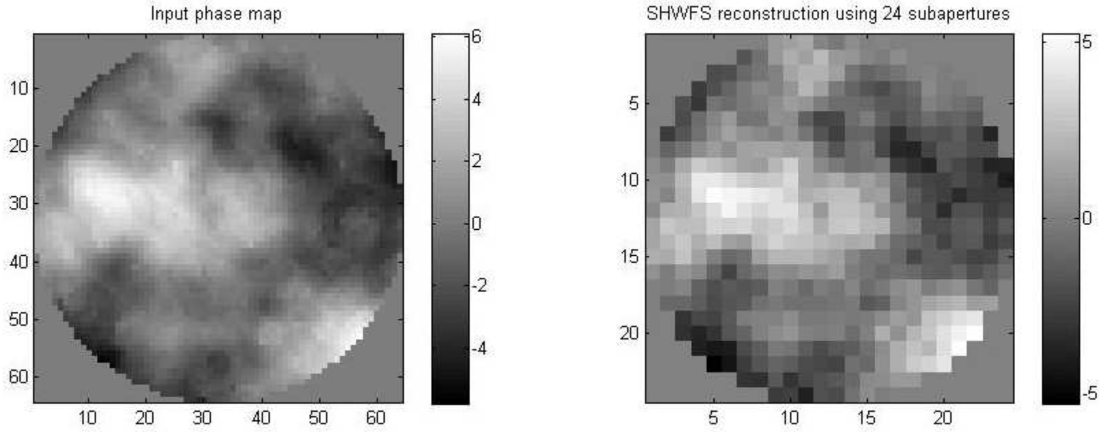

Fig. 3. Wavefront reconstruction using a 24 subaperture SHWFS.

aperture. For example there are 19 modes that correspond to 1 cpa, 32 modes that correspond to 2 cpa, 48 modes that correspond to 3 cpa, 64 modes that correspond to 4 cpa, 80 modes that correspond to 5 cpa, 96 modes that correspond to 6 cpa, 144 modes that correspond to 9 cpa, so on and so forth. Fourier reconstruction of the pupil plane phase with the nlCWFS is shown in Figure 4. Fourier reconstruction with the 16 subaperture SHWFS is shown in Figure 5, and with the 24 subaperture SHWFS is shown in Figure 6.

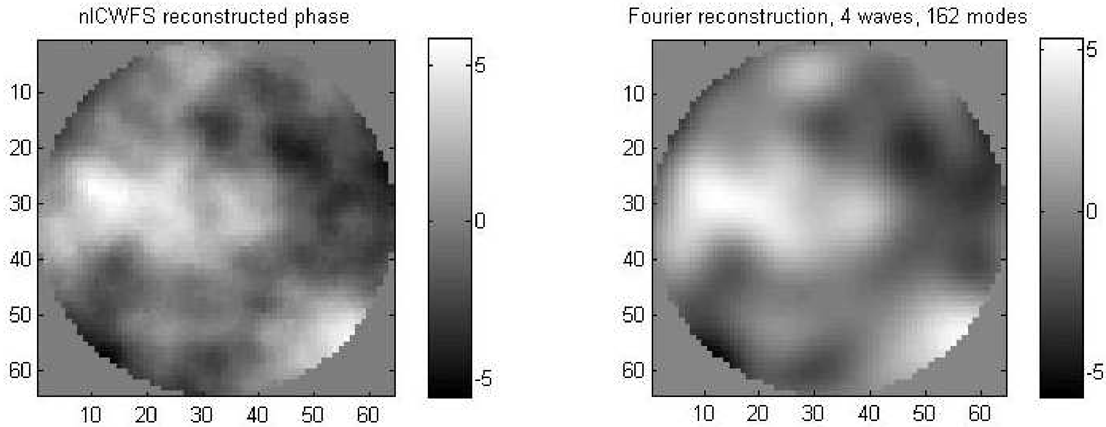

Fig. 4. Fourier reconstruction of the nlCWFS reconstructed phase. The first 4 spatial frequencies consisting of a total of 162 modes were used to reconstruct the phase.

3. Simulations and Sensitivity Analysis

We show results from simulations of the AFRL/RDS Optics Division 1.5 m telescope in which we compare a wavefront sensed by three WFS, a nlCWFS, a 16 subaperture SHWFS, and a 24 subaperture SHWFS. The simulations are open loop as our goal is to determine how sensitive the WFS is, and not necessarily to correct the wavefront. The simulation parameters are given in Table 1.

A Monte Carlo experiment was carried out in which the pupil phase reconstructed by each of the WFSs was decomposed into Fourier coefficients one hundred times with photon noise as the only parameter varying between iterations. The standard deviation or the error of each Fourier coefficient was determined over the 100 iterations and β was computed using the theoretical formula given in Eq. 1 [1].

$$\beta = \Sigma * \sqrt{N_{ph}} \tag{1}$$

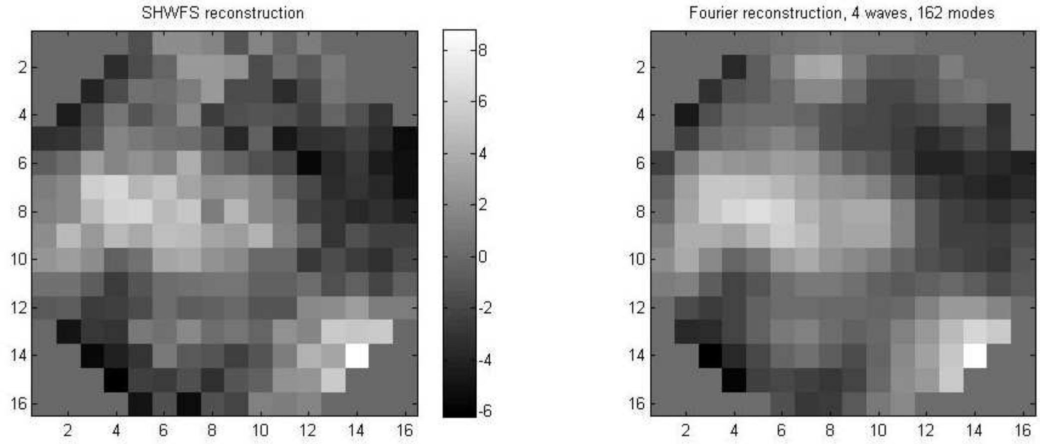

Fig. 5. Fourier reconstruction of the 16 subaperture SHWFS reconstructed phase. The first 4 spatial frequencies consisting of a total of 162 modes were used to reconstruct the phase.

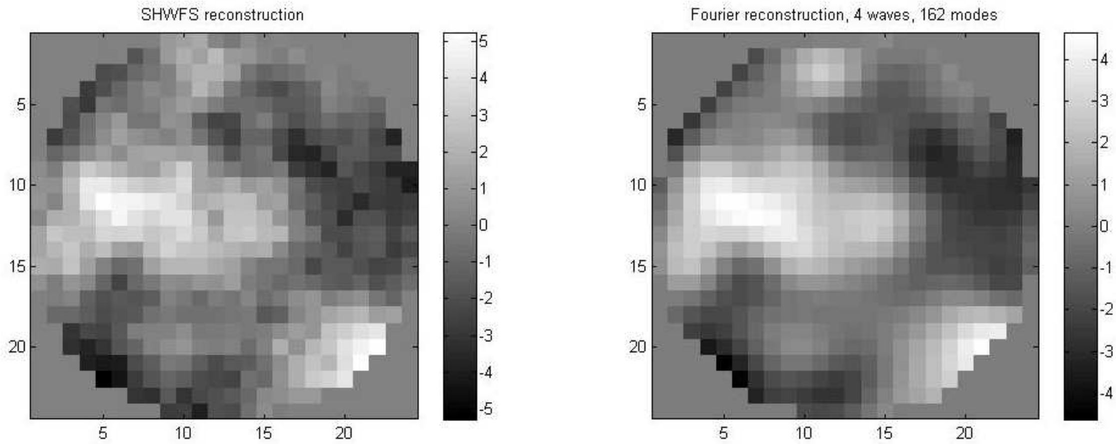

Fig. 6. Fourier reconstruction of the 24 subaperture SHWFS reconstructed phase. The first 4 spatial frequencies consisting of a total of 162 modes were used to reconstruct the phase.

Table 1. Default Parameters for Simulations

Parameter	nlCWFS	SHWFS
Telescope diameter	1.5 m	
WFS wavelength	790 nm	
Source brightness	$m_v = 20$	
Integration time	0.001 s	
Fried's coherence length	0.13 m @ 790 nm	
Greenwood frequency	$1.37\,\mathrm{s}^{-1}$	
WFS detector readout noise	0	
WFS detector quantum efficiency	1	
WFS subapertures	not applicable	16 & 24
Fresnel plane distances	-230 km, -114 km, 114 km, 230 km	not applicable
WFS detector sampling	64 pixels across pupil	4×4 pix. per subaperture
Spatial frequency control range	up to 16 CPA	up to 4 CPA & up to 6 CPA

here β defines the sensitivity of the wavefront sensor to each Fourier mode or spatial frequency, Σ is the error per mode and N_{ph} is the number of photons incident on the detector. For the nlCWFS photon noise was added at each Fresnel plane. In the simulations $100\,\%$ of the light reaches Fresnel plane 1, $95\,\%$ of the light reaches Fresnel plane 2, $90\,\%$ of the light reaches Fresnel plane 3, and $85\,\%$ of the light reaches Fresnel plane 4. In the case of the SHWFS photon noise is added at the single detector plane. The detectors are modeled to be noise free and have a quantumn efficiency of 1, therefore the only source of error is photon noise. Results from the Monte Carlo experiment is shown in Figure 7 where β is plotted as a function of the spatial frequency given in cycles per aperture. β represents the number of photons required by each WFS to reconstruct a given spatial frequnency. The combination of the reconstructed spatial frequencies allow us to reconstruct the wavefront in the pupil so that it can be corrected. A lower β implies that the WFS requires fewer photons to reconstruct the spatial frequency and is thus a more sensitive WFS. Our results show that, on average, the nlCWFS requires approximately $10\times$ fewer photons than the SHWFS to sense the first five spatial frequncies which means that a source that is dimmer by two magnitudes ($\Delta m_v = 2$) can be detected. Notice that, in Figure 7, the beta curve for the nlCWFS dips below 1 which is unphysical. This effect is due to mode coupling, which has been discussed in Section 2. In Figure 8 the values for the 16 subaperture SHWFS are not plotted as the 16 subaperture SHWFS does not have the resolution to accurately sense more than 4 CPA. The degradation in sensing is gradual but becomes significant at 6 CPA. According to Figure 8 the nlCWFS will be able to detect an object that is approximately $4\times$ dimmer than the detection limit of a 24 subaperture SHWFS. There is a difference in the values of the Fourier coefficents depending on how many spatial frequencies are used to reconstruct the phase map. This effect is also a result of mode coupling and needs to be investigated further.

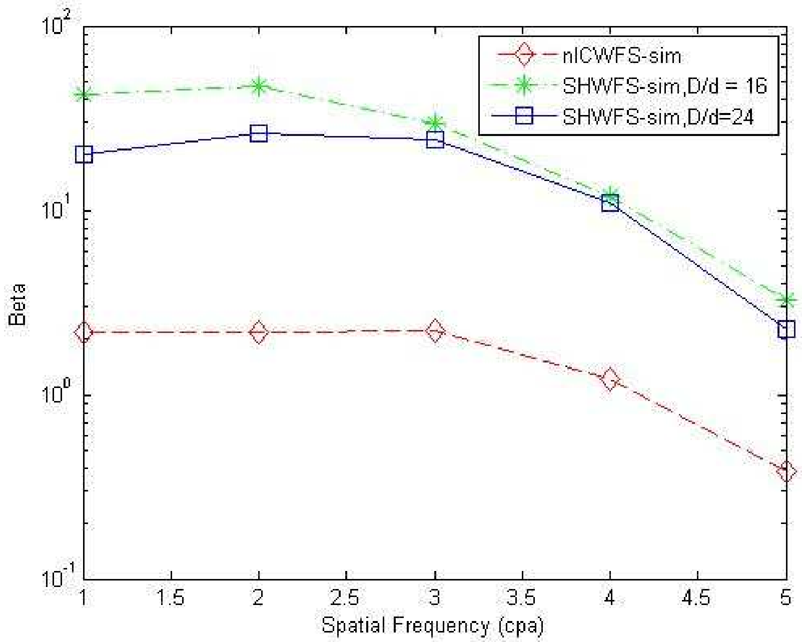

Fig. 7. WFS sensitivity as a function of spatial frequency. β plotted on the y-axis represents the square-root of the incident photons times the error per mode. β is a measure of the number of photons needed to reconstruct a spatial frequency for a given SNR. In this plot spatial frequencies of up to 5 cycles per aperture (cpa) are plotted. 5 cpa correspond to 80 Fourier modes.

4. Conclusion and Future Work

The simulations presented in this paper show that the nlCWFS is a more sensitive sensor compared to the SHWFS. Our results demonstrate that for a $1.5\,$m telescope the nlCWFS can detect an object that is at least two visible magnitudes dimmer than the current detection limit of the SHWFS. The sensitivity curves presented in Section 3 verify theoretical calculations that suggest that the nlCWFS is more sensitive to low order modes than the SHWFS. These low order aberrations dominate the atmospheric turbulence and scatter light on to dim planets that lie in close proximity to bright stars. In order to be able to detect the dim planet it is essential to sense and correct low order modes so that a high

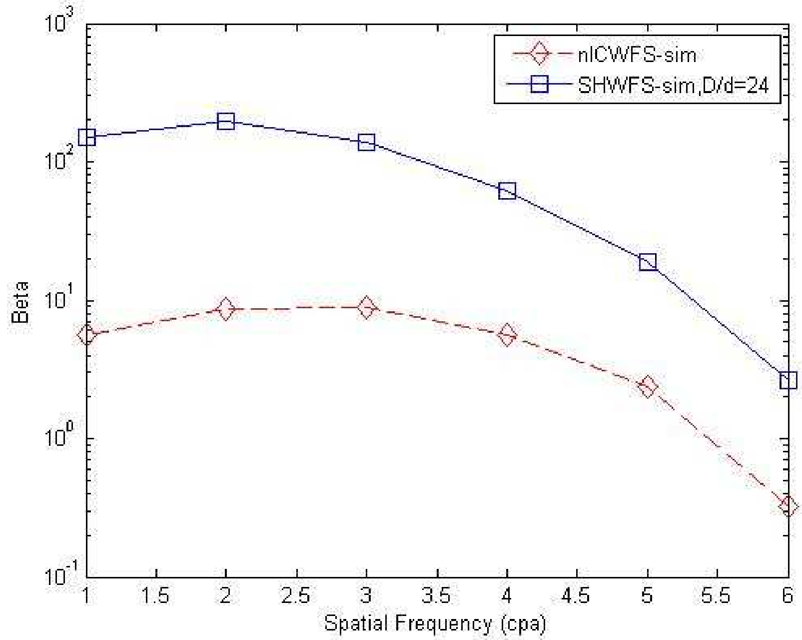

Fig. 8. WFS sensitivity as a function of spatial frequency. β plotted on the y-axis represents the square-root of the incident photons times the error per mode. β is a measure of the number of photons needed to reconstruct a spatial frequency for a given SNR. In this plot spatial frequencies of up to 6 cycles per aperture (cpa) are plotted. 6 cpa correspond to 96 Fourier modes.

contrast can be obtained between the star and the planet. Since the nlCWFS requires such few photons to reconstruct a set of spatial frequencies, it can operate without the use of a laser guide star (LGS). The use of a LGS in an adaptive optics (AO) system is both expensive and labor intensive as it requires the obtaining of permission to lase, and people to monitor the lasing field of view to ensure that it is free of air crafts. Therefore the ability to sense and correct without the use of LGS will be a welcome AO development.

Since Fourier modes are not orthogonal on a circular aperture we see the effects of mode coupling on the amplitudes of the Fourier coefficients. Further work needs to be done to establish a relationship between the input phase and the decomposed Fourier coefficients. There seems to be a non-linear correlation between the number of coefficients corrected and the resulting coefficient amplitudes, which needs to be investigated. In the past we have built two nlCWFSs for the 6.5 m MMT AO system, with modified optical designs. Based on the lessons learned from observing with both the previous instruments we have an optimal design for the AFRL/RDS Optics Division 1.5 m telescope. In the coming year we hope to complete the optical design and begin integrating with the 1.5 m telescope.

5. ACKNOWLEDGMENTS

The authors would like to thank the Air Force Research Lab for supporting this research and Dr. Earl Spillar for valuable comments.

References

1. O. Guyon. Limits of Adaptive Optics for High-Contrast Imaging. *Astrophys. J.* , 629:592–614, August 2005.
2. M. Mateen, O. Guyon, M. Hart, R. Johnson, and E. Spillar.
3. M. Mateen, V. Garrel, M. Hart, and O. Guyon. Results from the laboratory demonstration of the nonlinear curvature wavefront sensor. In *Society of Photo-Optical Instrumentation Engineers (SPIE) Conference Series*, volume 7736 of *Society of Photo-Optical Instrumentation Engineers (SPIE) Conference Series*, July 2010.
4. O. Guyon. High Sensitivity Wavefront Sensing with a Nonlinear Curvature Wavefront Sensor. *PASP*, 122:49–62, January 2010.
5. R. W. Gerchberg and W. O. Saxton. A practical algorithm for determination of the phase from image and diffraction planes. *Optik*, 35:237–246, December 1972.